arXiv:astro-ph/0406413v1 18 Jun 2004

The Distribution of Lyα-Emitting Galaxies at z=2.38: Paper 2, Spectroscopy

Paul J. Francis[1]

Research School of Astronomy and Astrophysics, the Australian National University, Canberra 0200, Australia

pfrancis@mso.anu.edu.au

Povilas Palunas

McDonald Observatory, University of Texas, Austin, TX 78712

Harry I. Teplitz

Spitzer Science Center, California Institute of Technology, Mail Code 220-62, 770 South Wilson Avenue, Pasadena, CA 91125

Gerard M. Williger

Dept. of Physics and Astronomy, Johns Hopkins University, 3701 San Martin Drive, Baltimore, MD 21218

and

Bruce E. Woodgate

NASA Goddard Space Flight Center, Code 681, Greenbelt, MD 20771

ABSTRACT

In Paper 1 of this series we identified an 80 co-moving Mpc filament of candidate Lyα emitting galaxies at redshift 2.38. In this paper we present spectroscopy of the 37 galaxy candidates. Our spectroscopy reached a surface brightness limit of 5.0×10^{-17}erg cm^{-2}s^{-1}arcsec^{-2}. Of the 14 candidates down to this limit, 12 were confirmed to be Lyα emitting galaxies at the filament redshift. We also obtained spectral confirmation for six of the lower surface brightness candidates, all of which also lay at the filament redshift. In addition, we identify a foreground cluster of QSOs at $z = 1.65$.

[1]Joint Appointment with the Department of Physics, Faculty of Science, the Australian National University

Subject headings: Large-scale structure of universe — galaxies: clusters — galaxies: high redshift — quasars: general

1. Introduction

A large fraction of galaxies today lie in filamentary structures, such as the Great Wall (Geller & Huchra 1989), separated by voids. When did these structures form? There are now some tentative observations suggesting that this topology was already in place as early as redshift three (eg. Campos et al. 1999; Møller & Fynbo 2001).

We recently carried out a large scale survey to measure the topology of the distribution of Lyα emitting galaxies at $z \sim 2.38$ (Palunas et al. 2004, hereafter Paper 1). We searched for candidate Lyα emitting galaxies in an 80$\times$ 80 $\times$ 60 co-moving Mpc region, using the now well established narrow-band selection technique (eg. Hu & McMahon 1996; Steidel et al. 2000; Kudritzki et al. 2000; Venemans et al. 2002; Rhoads et al. 2003; Ouchi et al. 2003; Stanway et al. 2004). The region was imaged through a narrow-band (54Å) filter, centered at 4110Å. This was sensitive to Lyα emitting galaxies at $2.36 < z < 2.40$. 37 candidate galaxies were found.

These candidate $z \sim 2.38$ galaxies mostly lie in a filamentary structure, over 80 co-moving Mpc in length. This filament is seemingly bracketed by voids on both sides. In Paper 1 we argue that this structure is statistically significant, and that the size of the voids and the filament is larger than would be expected from CDM (Cold Dark Matter) simulations.

We did not, however, have spectra of the candidate high redshift galaxies. It was thus possible that some or all of them were actually foreground galaxies: galaxies lying at $z \sim 0.1$ whose O II 3727Å line lies within the filter bandpass. Even if they were Lyα emitting galaxies at $z \sim 2.38$, their observations only constrained the two dimensional position of the galaxies and not their precise redshift.

In this paper, we present confirmation spectroscopy of these galaxy candidates. We demonstrate that candidates are indeed primarily $z \sim 2.38$ Lyα emitting galaxies, and we constrain the three-dimensional shape of the claimed filament.

2. Observations and Reduction

Our spectroscopy was carried out using the Two Degree Field (2dF) multi-fiber spectrograph on the Anglo-Australian Telescope (AAT, Lewis et al. 2002). This spectrograph has 400 fibers, spread over a circular field of diameter two degrees, located at the prime focus of the AAT.

Fibers were allocated to targets using the *configure* program (Lewis et al. 2002). First priority in the fiber allocation was given to the candidate z=2.38 galaxies identified by Palunas et al. (2004) (the main sample). We were able to allocate fibers to all but two of these (the two unobserved sources, those at 21:40:33.1 -44:36:10.8 and 21:43:05.9 -44:27:21.0, J2000, lay too close to other candidate galaxies for fiber allocation). Second priority was 26 brighter point sources which also showed excess narrow-band flux: these were potential z=2.38 QSOs. Three of these were too bright for us to observe, but we were able to allocate fibers to twenty of the remaining twenty-three (the point source sample).

The candidate list of Palunas et al. (2004) only included sources with excess narrow-band emission of equivalent width > 125Å. This was done to minimize contamination from foreground [O II] emitting galaxies, but may also have eliminated some Lyα emitting sources. To check this, we selected a sample of 86 sources which showed excess emission in the narrow band, but not enough to meet this equivalent width threshold (the low equivalent width sample). We were able to allocate fibers to 70 of these sources.

211 UVX sources were selected, as possible foreground QSOs. We were able to allocate fibers to 120 of these (the UVX sample). Four candidate color-selected high redshift QSOs were also observed.

Fibers were allocated to 17 Chandra sources: these will be discussed by Williger et al (in preparation).

2.1. Observations

Observations were carried out on the nights of 2003 August 31 and September 1. Conditions were poor: the first night was mostly cloudy, and the second night, while clear, suffered from $\sim 2.5''$ seeing. We obtained a total integration time of 5400 sec on the first night and 32,400 sec on the second night, though much of this was obtained at high airmass, or while the moon was up.

The first night's data were reduced quickly, allowing us to identify several foreground galaxies amongst the low equivalent width sample. The fiber configuration was changed for

the second night by eliminating these sources, allowing us to observe more of the various lower priority samples. This also means that the higher priority sources were observed through different fibers on the different nights, giving us a check against systematic errors.

We used the 600V gratings in both the 2dF spectrographs, centered at a wavelength of 4982Å. This gave a spectral resolution of 450 km s^{-1} and a wavelength range of 3890 – 6080Å. The data were reduced using the *2dfdr* software (Lewis et al. 2002).

Spectra from each night were co-added separately, as a check on the reality of any faint features seen. A weighted sum of the spectra from both nights was then used in the final analysis.

2.2. Spectral Classification

All spectra were classified interactively. For sources showing a single narrow emission line at $\sim$ 4110Å, we classified them either as $z \sim 2.38$ Lyα emitting galaxies or $z \sim 0.1$ [O II] emitting blue compact galaxies using the following criteria:

- If we see corresponding [O III] and/or Hβ emission lines, we identify the source as an [O II] emitting galaxy at $z \sim 0.1$.
- If we see corresponding C IV emission line, we identify the source as a Lyα emitting galaxy at $z \sim 2.38$.
- If the $\sim$ 4110Å line has a velocity width $>$ 500km s^{-1}, and no other lines are seen, we classify the line as Lyα at $z \sim 2.38$, on the basis that the [O II] emission of a blue compact galaxy is unlikely to be this broad.
- The remaining three sources (with single narrow lines) were classified as Lyα emitting galaxies at $z \sim 2.38$, on the basis that had they been at $z \sim 0.1$, we should have been seen [O III] emission (our $z \sim 0.1$ galaxies have a median flux calibrated ratio of [O III]/[O II]= 1.7). One of these three was confirmed by Francis, Woodgate & Danks (1997) to lie at $z \sim 2.38$.

The detection of an emission-line is regarded as secure if it is seen at greater than 5σ confidence. If seen at between 3 and 5 σ confidence, it is regarded as marginal.

3. Results

3.1. The Main Sample

We were able to obtain secure spectral classifications for most sources down to an emission-line surface brightness $> 5.0 \times 10^{-17}$erg cm^{-2}s^{-1}arcsec^{-2}. We observed 14 candidates down to this limit. 10 were securely classified as $z \sim 2.38$ Lyα emitting galaxies, and two more were marginally confirmed as the same. One of the remaining sources was the bizarre B5, discussed below, and the other showed clear stellar absorption and is hence a foreground source. Three of the securely confirmed sources had previous spectral confirmation (Francis, Woodgate & Danks 1997).

At fainter surface brightnesses our sucess rate was lower. Of the 21 remaining sources we observed, we were only able to obtain a secure spectral classification for 6, and a marginal classification for another 9. All were classified as $z \sim 2.38$ Lyα emitting galaxies. No spectral features were detected in the remaining 6 sources.

We show spectra of the securely confirmed $z \sim 2.38$ Lyα emitters in Fig 1, and list their properties in Table 1. Those with only marginally (3 – 5σ) detected Lyα lines are shown in Fig 2 and their properties listed in Table 2.

Composite spectra of all sources classified as $z \sim 2.38$ Lyα emitting galaxies were constructed (Figs 3 & 4) by shifting the spectra to align the centroid of the putative Lyα line at a nominal wavelength of 1216Å. If a significant fraction of these sources were foreground [O II] emitting galaxies, we would expect to see Hβ and [O III] in these composite spectra, shifted to 1585Å and 1633Å respectively. Nothing is seen at these wavelengths: instead C IV is weakly detected in the composite of the securely confirmed sources.

A close-up of the Lyα region of these composite spectra (Fig 5) does not show evidence of asymmetry in the profiles. The individual spectra are too poor to check for asymmetry, though in our previous spectrum of B1, strong asymmetry was seen (Francis et al. 1996). This does not rule out a systematic asymetry in these lines, as it could have been washed out by centroiding errors in these noisy spectra. We are unable to look for evidence of a continuum break across the Lyα line due to the difficulty in accurately sky-subtracting 2dF spectra.

One source, B5 (coordinates 21:43:03.57 -44:23:44.2, J2000), proved impossible to classify. B5 is one of the most luminous narrow-band excess sources, and in Paper 1 we classified it as a Lyα blob. Our image of it shows that the excess narrow-band flux is centrally concentrated, but clearly extended. Our spectrum (Fig 7) shows two clear broad emission lines: one at 4110Å and the other at 5930Å. Both lines, though noisy, are independently seen in the

co-added data from each night, and must therefore be regarded as secure. A more marginal candidate broad line is possibly seen at 4440Å. The breadth of the lines ($\sim$ 4000km s^{-1}) clearly indicates that this is a QSO. The fact that B5 shows extended narrow-band fuzz suggests that the line at 4110Å is either Lyα or [O II]. If the former, however, the 5930Å line would have a rest-frame wavelength of $\sim$ 1750Å, which does not correspond to any normal QSO emission line (Francis et al. 1991). If the latter, we do not see any Balmer lines or [O III], and the 5930Å line would lie at rest-frame 5390Å; another wavelength which does not correspond to any strong QSO line. No alternative identification of the lines works any better. A higher quality spectrum with wider wavelength coverage is clearly needed.

Three of the securely confirmed $z \sim 2.38$ galaxies show significant C IV in emission. Two of these (B38 and B39) have Lyα velocity widths greater than 1000km s^{-1} and are thus probable QSOs. The remaining source (B23), while its Lyα emission is relatively narrow (800km s^{-1}) appears to have much broader C IV emission. These sources may thus all be QSOs, albeit width host galaxy light contributing to their spatially extended images.

Our spectroscopy thus demonstrates that down to a narrow-band flux surface brightness limit of 5.0×10^{-17}erg cm^{-2}s^{-1}arcsec^{-2}, the vast majority of our candidates are indeed Lyα emitting galaxies at $z \sim 2.38$. There is nothing in our data to suggest that this fraction is not comparable for the fainter sources, but deeper data will be required to confirm this.

3.2. Other Samples: QSOs and Foreground Galaxies

Thirteen of the twenty point source sample objects observed were QSOs with a broad emission line within the narrow-band filter bandpass. Only one of these, however, (Fig 3) was at the filament redshift: ten lie at $z \sim 1.65$ which places C IV within the passband. The other two lie at z=0.457 and z=1.458, placing Mg II and He II respectively in the passband. Two of the remaining sources had no significant features in their spectra, and the other two were low redshift compact emission-line galaxies (one with [O II] in the passband).

A further 41 QSOs were found in the UVX sample, and three in the low equivalent width sample. Three of the UVX QSOs lie at higher redshifts than our candidate filament, and are shown in Fig 6. All QSOs identified are listed in Table 3. Given our restricted wavelength coverage, we often see only a single emission line: these one line sources are noted in the table, and given redshifts typically assuming that this line is Mg II. QSOs with lines only marginally detected are indicated with question marks.

We detect 19 galaxies whose redshifts place [O II] within the passband of our filter. These, together with other foreground emission-line galaxies, are listed in Table 4.

4. Discussion

4.1. Are the Filament and the Voids Real?

In Paper 1, we showed that the two-dimensional positions of the candidate $z \sim 2.38$ galaxies on the sky was non-random, and that the two-dimensional void probability function measured from these candidates was marginally inconsistent with one set of cold dark matter simulations.

We repeated this analysis, adding in the confirmed $z \sim 2.38$ QSO but removing the confirmed foreground source. This made no appreciable difference to the results from Paper 1. We then repeated the analysis using only those candidates with secure spectral confirmation, and again combining these with the marginally confirmed candidates. Both analyses gave results consistent with those in Paper 1, but with larger error bars. In neither case, however, was the measured void probability function inconsistent with the cold dark matter simulations with 95% confidence. The three-dimensional distribution of the galaxies is discussed in § 4.2.

We show in § 3.1 that for sources above our surface brightness limit, at least 70% lie at $z \sim 2.38$. We further show that there is no spectral evidence that any of the main sample sources are foreground [O II] emitting galaxies at $z \sim 0.1$. A further test for any population of foreground interlopers is the distribution of our candidates on the sky. In Fig 8 and Fig 9, we show that the projected distribution of confirmed foreground $z \sim 0.1$ galaxies is quite different from that of the candidate $z \sim 2.38$ galaxies, being concentrated on the cluster Abell 3800 (Abell, Corwin & Olowin 1989).

Fig 9 also demonstrates that the sources for which we have secure spectral confirmations are scattered throughout the cliamed filament, rather than all being gathered in one region. There is a relative deficit of securely confirmed sources in the center of the filament, but the three confirmed sources that do lie in this region were those studied by Francis, Woodgate & Danks (1997), all of which have secure multi-line spectroscopic confirmation. The redshifts of the sources at the top and bottom of the filament show no significant differences, so there is no evidence in this data set for the filament being simply two clusters with a few stray sources lying between them, though this model cannot be ruled out.

4.2. Is it a Filament or a Sheet?

If the putative filament were inclined to our line of sight, we might expect to see a redshift gradient along it, as was seen by Møller & Fynbo (2001) in their much smaller

filament. No such correlation was seen: a plot of Lyα wavelength against position along the filament contains neither a gradient nor any sub-structure.

The distribution of all Lyα redshifts is shown in Fig 10. The mean redshift (including both secure and marginal candidates) is $z = 2.3791$, with a standard deviation of 820km s^{-1}. The corresponding figures for sources with secure redshifts only are $z = 2.3807$ and 800km s^{-1}.

The standard deviation in the observed redshifts is comparable to the average Lyα line width of the individual galaxies (860km s^{-1}, or 730km s^{-1} if we subtract in quadrature the instrumental resolution, Table 1). As the Lyα line is probably extremely optically thick, one would expect the observed line peak to be offset from the true systemic redshift by of order the line width. Thus the scatter in the observed redshifts may be purely an artifact of the optical depths: we have no significant evidence for an intrinsic scatter. Measurement of the velocity structure will require observations in a line less optically thick.

Are we really seeing a concentration of sources at a particular wavelength, or is the measured wavelength dispersion simply an artifact of the bandpass of our selection filter? Fig 10 suggests that the observed redshift distribution is more sharply peaked than the filter bandpass, and that the peak lies at a slightly longer wavelength. We tested this by Monte-Carlo simulating samples of randomly distributed galaxies observed through this filter, assuming a Lyα luminosity function with $N(L) \propto L^{-0.87}$, as used in Palunas et al. (2004). Slightly fewer than 0.1% (0.6% for secure sources only) of the simulations have measured velocity dispersions as low as we obtained.

The statistical difference is mostly driven by the relative lack of observed lines lying in the wavelength range 4085 — 4105Å: ie. the observed galaxy distribution has a lower redshift cut-off. But does it have a higher redshift cut-off, or is the lack of observed galaxies with Lyα wavelengths longer than around 4125Å caused only by the filter bandpass? Once again, we tested this using our Monte-Carlo simulations. Slightly fewer than 1% of simulations having the same sample size as the combined secure and marginal samples had as few sources long-ward of 4125Å as we saw, but if we restrict ourselves to sources with secure spectral classifications only, this fraction rises to 10%.

We conclude that we are probably looking at a filament viewed from within $\sim 30^\circ$ of sideways, rather than an edge-on sheet. There remains a small possibility that it is a sheet but that we are only sampling its front edge, as we do not definitively detect a higher redshift cut-off.

4.3. QSO Clusters

Only one QSO was found in the point source sample at the filament redshift: would we have expected more? In the point source sample, we are effectively finding QSOs down to $B \sim 21.8$. Extrapolating the QSO luminosity functions of Boyle et al. (2000), allowing for QSOs to be selected in our narrow-band filter even if only part of their broad Lyα emission is within the filter bandpass and for our incomplete spectroscopy, we would expect 0.75 QSOs to have been found, if the region studied was not overdense in them. Thus the observations are quite consistent with this region being average.

In Paper 1 we reported that the filament region had an overdensity of Lyα emitting galaxies of $\times 4$. Is this consistent with the observation of only one QSO? Using Poisson statistics, if the region were overdense by a factor of 4, we'd find one or fewer QSOs 20% of the time. Thus finding only one QSO is consistent with such an overdensity, though favoring lower values.

Perhaps the greatest surprise is the 10 QSOs identified with $1.61 < z < 1.69$, which places some or all of their C IV emission in the narrow-band filter. From the Boyle et al. (2000) luminosity functions, we'd predict only 1.8 QSOs in this range. The Poisson probability of finding 10, if the field were not overdense, is only 0.5%. We therefore conclude that a cluster of QSOs lies in the foreground of our field at $z = 1.65$. Note that all ten were identified by their UVX emission as well as their excess narrow-band flux.

In Fig 11 we show the distribution of these QSOs. It is clearly non-random: they are concentrated into the South-East corner of the field. The overdensity of QSOs within this region is > 3 with 95% confidence.

Could gravitational lensing by this cluster, plus Abell 3800, be responsible for the filament and voids seen at z=2.38? Cluster lensing could certainly be amplifying a handful of individual sources, but expected magnifications over the enormous extent of our field are insignificant.

5. Conclusions

The spectroscopy presented here demonstrates that the brighter candidate filament members do indeed lie at redshift 2.38, and that the candidate list is not extensively contaminated by $z = 0.1$ interlopers. We can also tentatively conclude that the galaxies we see do indeed lie in a one-dimensional filament, and not a slice through some two dimensional sheet. These results lend credence to our claim (in Paper 1) that galaxies at high redshifts

are distributed in filaments separated by voids. A definitive test of this claim will, however, require the systematic mapping of more and larger volumes of the high redshift universe.

Curiously, the filament region is not overdense in QSOs, but we find a significant cluster of foreground QSOs at $z \sim 1.65$. One QSO was found lying within the filament, as were three background QSOs. Follow-up spectroscopy of these QSOs may allow us to constrain the gas within the filament and voids, as has already been done for the three background QSOs previously known (Francis & Williger 2004).

This study was funded by a NASA grant NRA–98–03–UVG–011, and supported by the STIS IDT through the National Optical Astronomical Observatories and by the Goddard Space Flight Center.

REFERENCES

Abell, G.O., Corwin, H.G. & Olowin, R.P. 1989, ApJS, 70, 1

Boyle, B.J., Shanks, T., Croom, S.M., Smith, R.J., Miller, L., Loaring, N. & Heymans, C. 2000, MNRAS, 317, 1014

Campos, A., Yahil, A., Windhorst, R.A., Richards, E.A., Pascarelle, S., Impey, C., & Petry, C. 1999, ApJ, 511, L4

Francis, P.J., Hewett, P.C., Foltz, C.B., Chaffee, F.H., Weymann, R.J. & Morris, S.L. 1991, ApJ, 373, 465

Francis, P.J. & Williger, G.M. 2004, ApJ, 602, 77

Francis, P.J., Woodgate, B.E. & Danks, A.C. 1997, ApJ, 482, 25

Francis, P.J. et al. 1997, ApJ, 457, 490

Geller, M.J. & Huchra, J.P., 1989, Science, 246, 897

Hu, E.M. & McMahon, R.G. 1996, Nature, 382, 231

Kudritzki, R.-P., Méndez, R.H., Feldmeier, J.J., Ciardullo, R., Jackoby, G.H., Freeman, K.C., Arnaboldi, M., nCapaccioli, M., Gerhard, O. & Ford, H.C. 2000, ApJ, 536, 19

Lewis, I.J. et al. 2002, MNRAS, 333, 279

Møller, P., & Fynbo, J. U. 2001, A&A, 372, L57

Ouchi, M. et al. 2003, ApJ, 582, 600

Palunas, P., Teplitz, H.I., Francis, P.J., Williger, G.M. & Woodgate, B.E. 2004, ApJ 602, 545 (Paper 1)

Rhoads, J.E., Dey, A., Malhotra, S., Stern, D., Spinrad, H., Jannuzi, B.T., Dawson, S., Brown, M.J.I. & Landes, E. 2003, AJ, 125, 1006

Stanway, E.R. et al. 2004, ApJ, 604, L13

Steidel, C.C., Adelberger, K.L., Shapley, A.E., Pettini, M., Dickinson, M, & Giavalisco, M. 2000, ApJ, 532, 170

Venemans, B.P., Kurk, J.D., Miley, G.K., Röttgering, H.J.A., van Breugel, W., Carilli, C.L., Ford, H., Heckman, T., McCarthy, & Pentericci, L., 2002, A&A, 361, 25

This preprint was prepared with the AAS LaTeX macros v5.2.

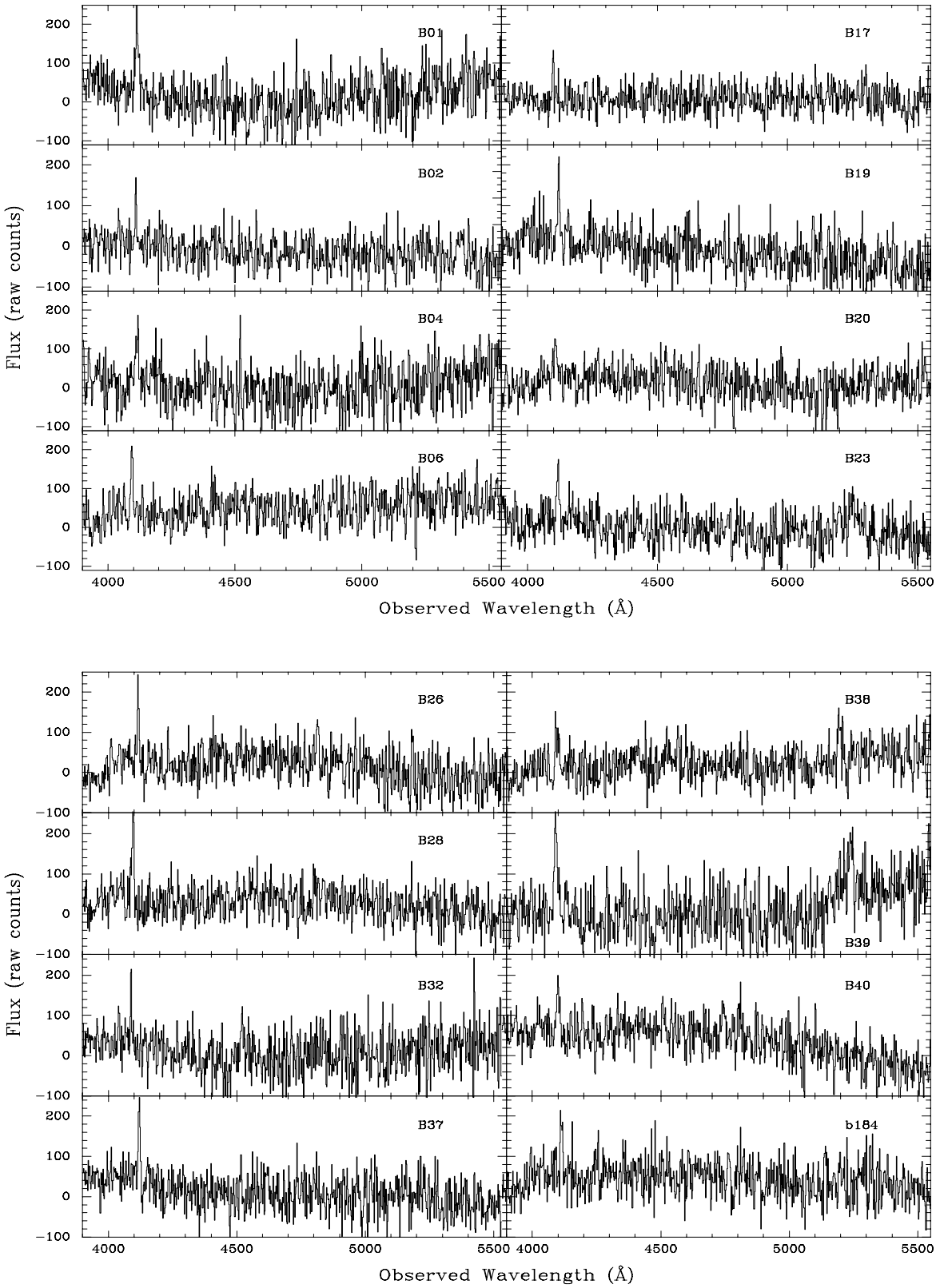

Fig. 1.— Spectra of confirmed ($> 5\sigma$) z=2.38 Lyα emitting galaxies. The spectra are not flux calibrated.

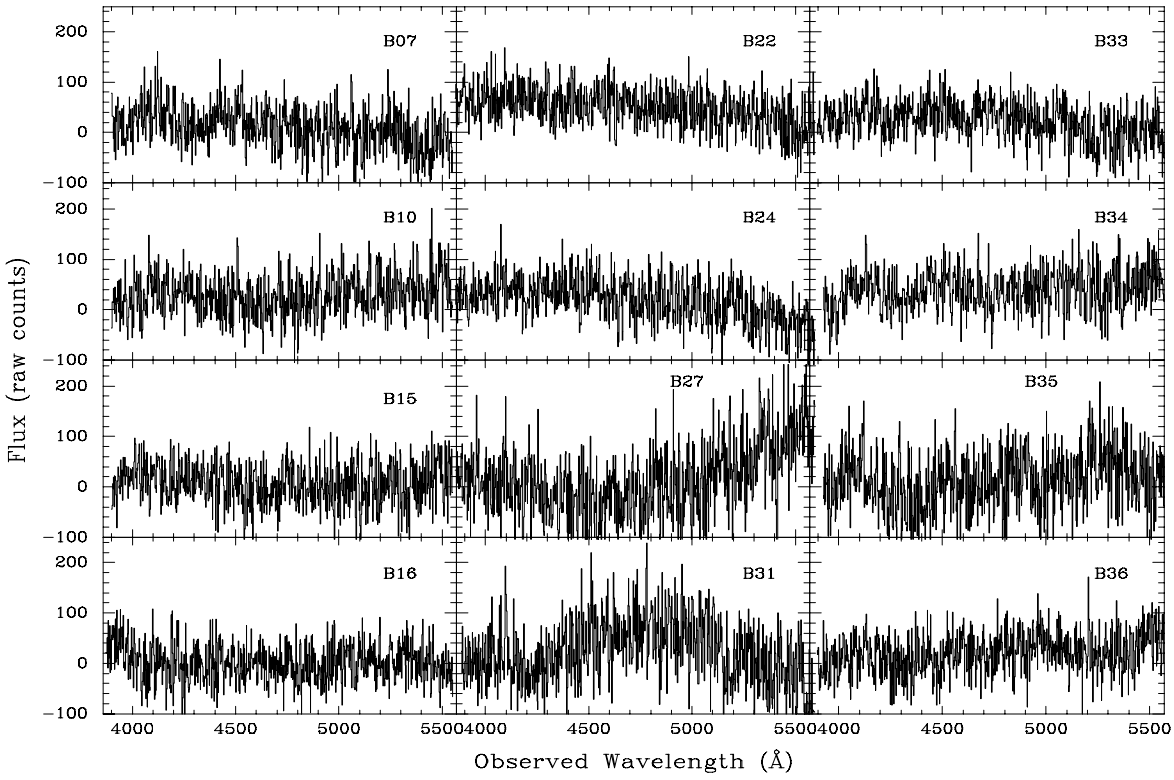

Fig. 2.— Spectra of the marginal (3 – 5 σ) z=2.38 Lyα emitting galaxy candidates. The spectra are not flux calibrated.

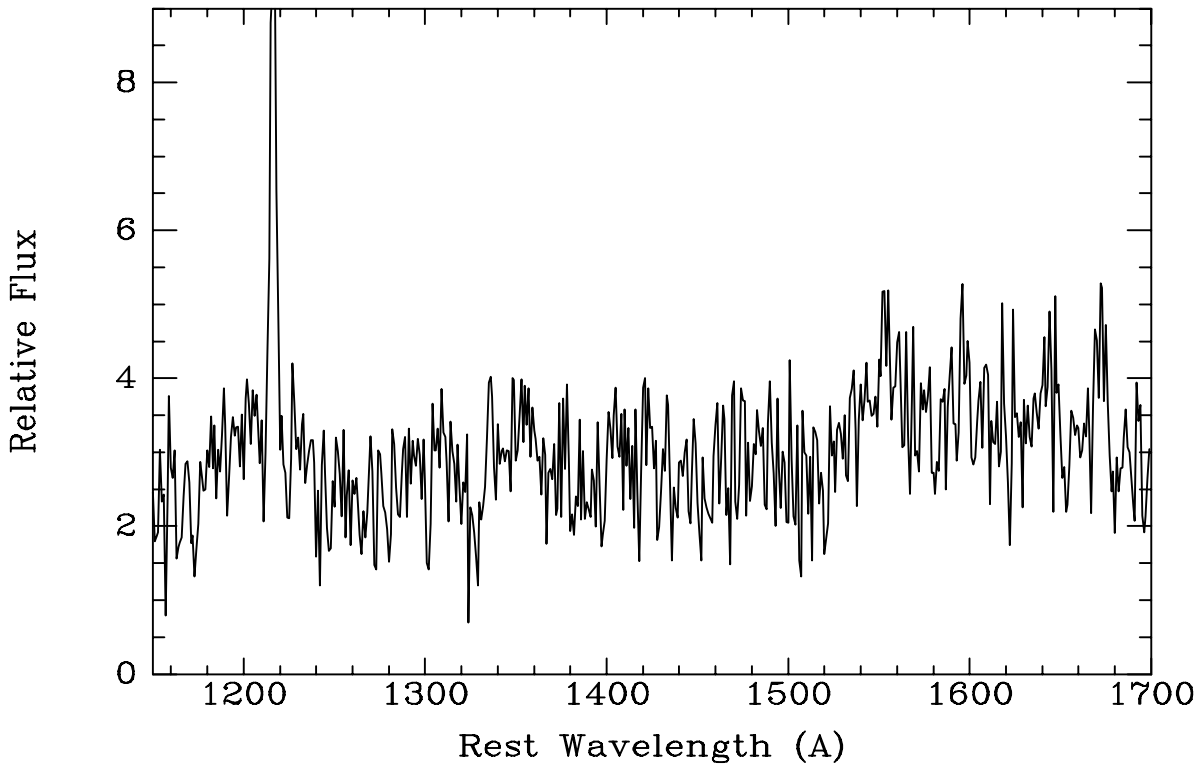

Fig. 3.— Coadded spectrum of the candidate $z \sim 2.38$ galaxies with a securely detected Lyα line.

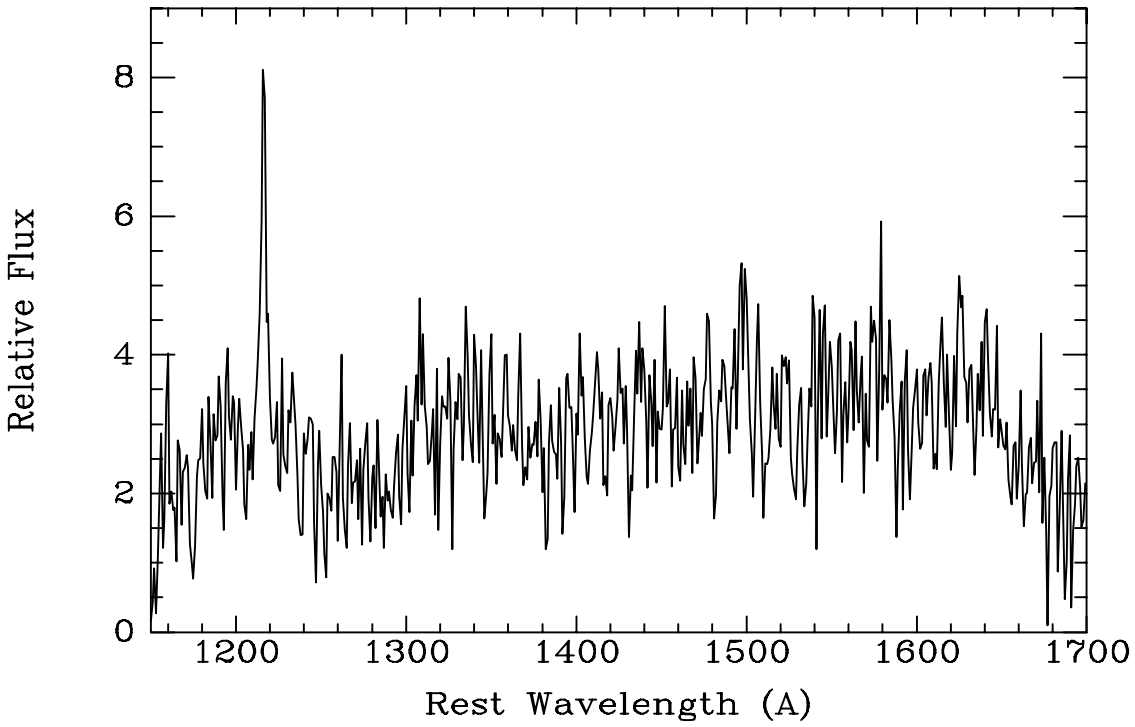

Fig. 4.— Coadded spectrum of the candidate $z \sim 2.38$ galaxies with a marginally detected Lyα line.

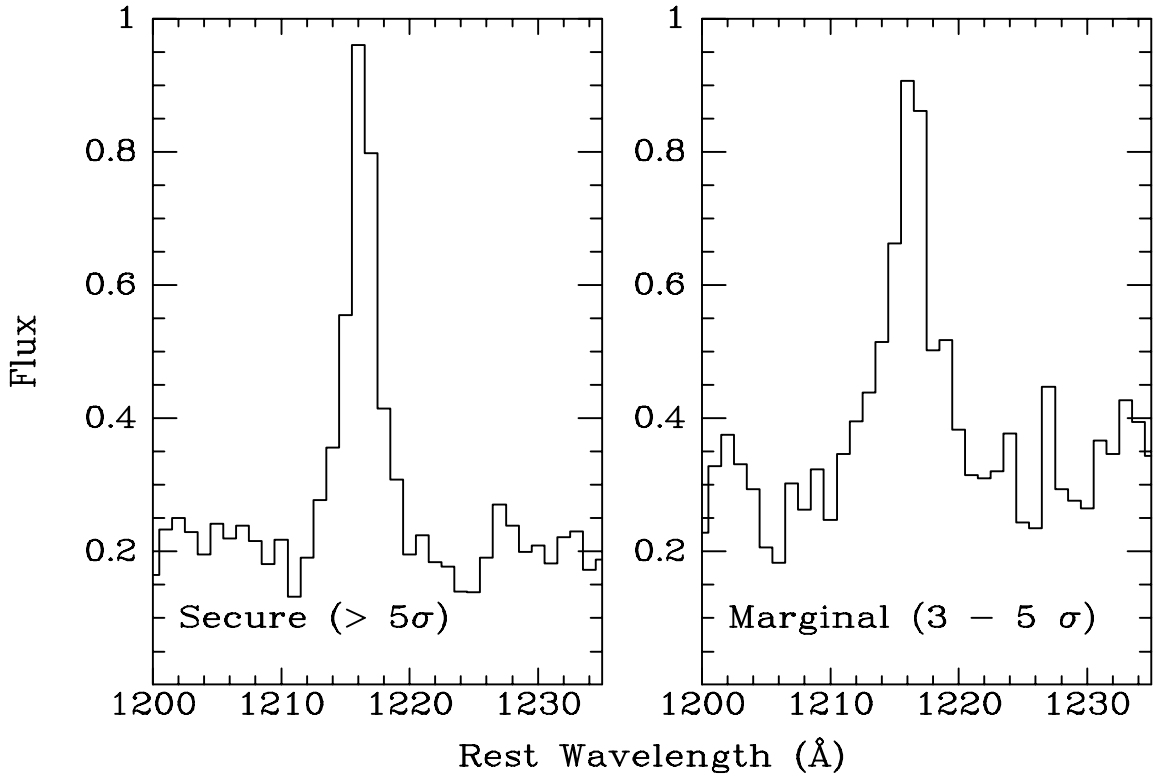

Fig. 5.— Close-up of the Lyα wavelength region of the two composite spectra in the previous two figures

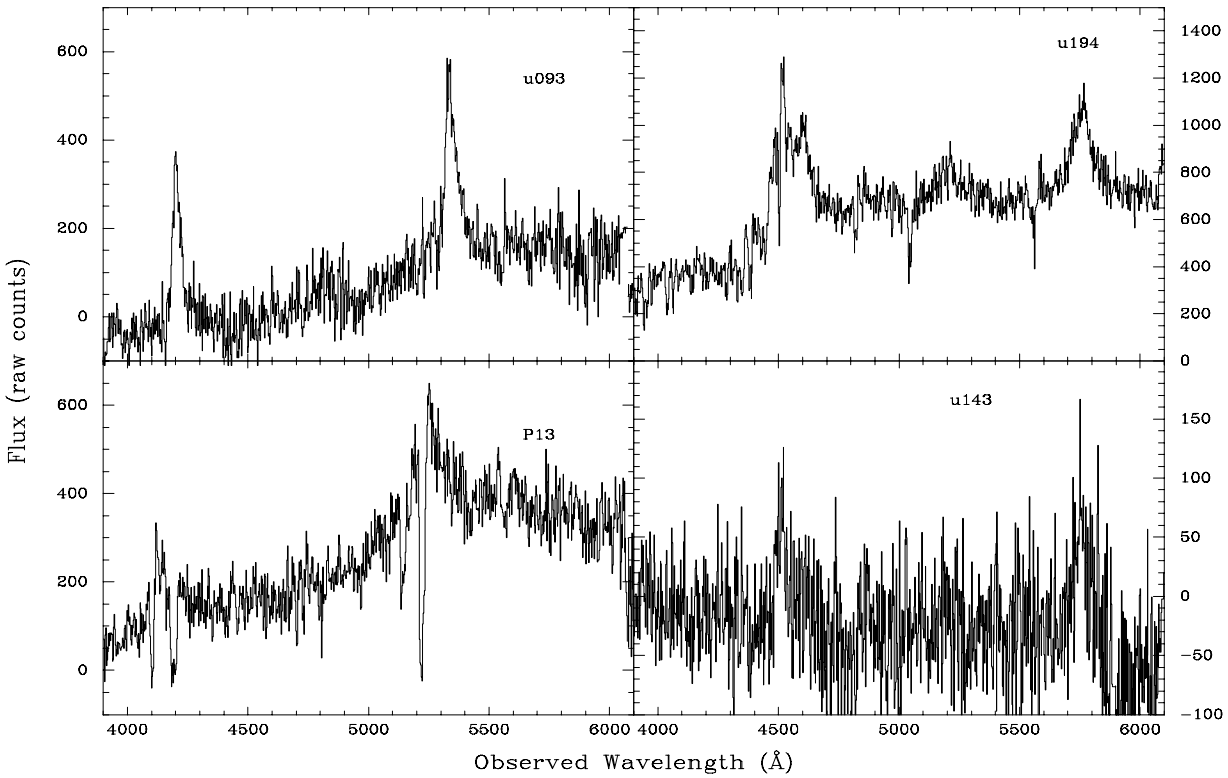

Fig. 6.— Spectra of QSOs lying at or behind the filament redshift. The spectra are not flux calibrated.

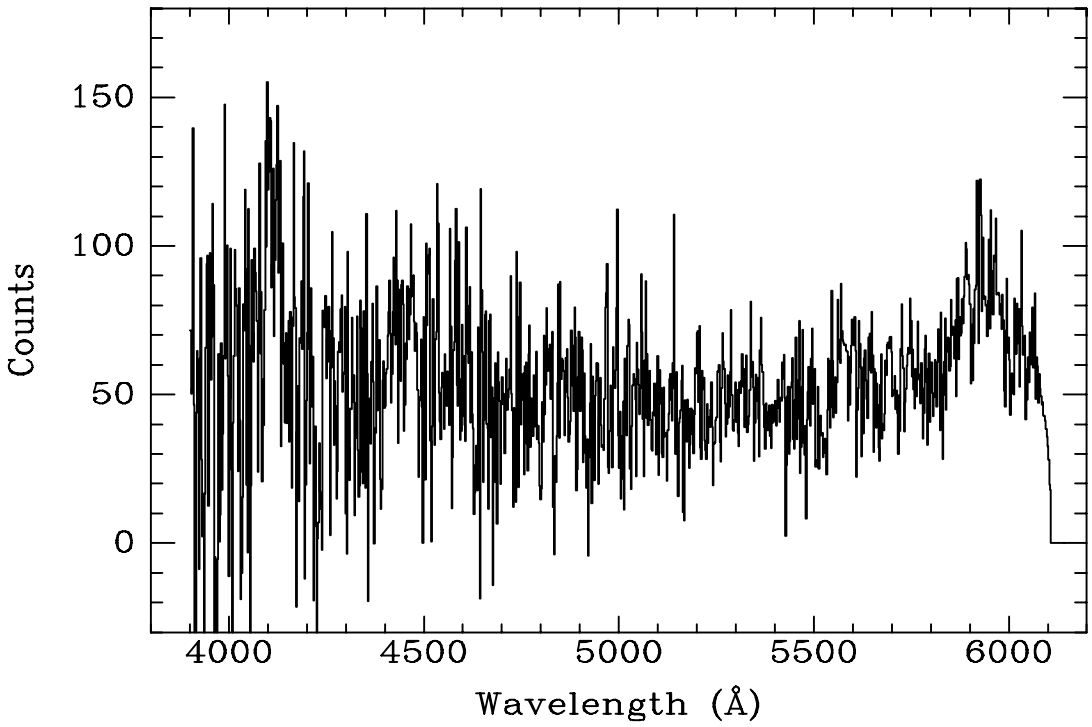

Fig. 7.— Spectrum of B5. The spectrum is not flux calibrated.

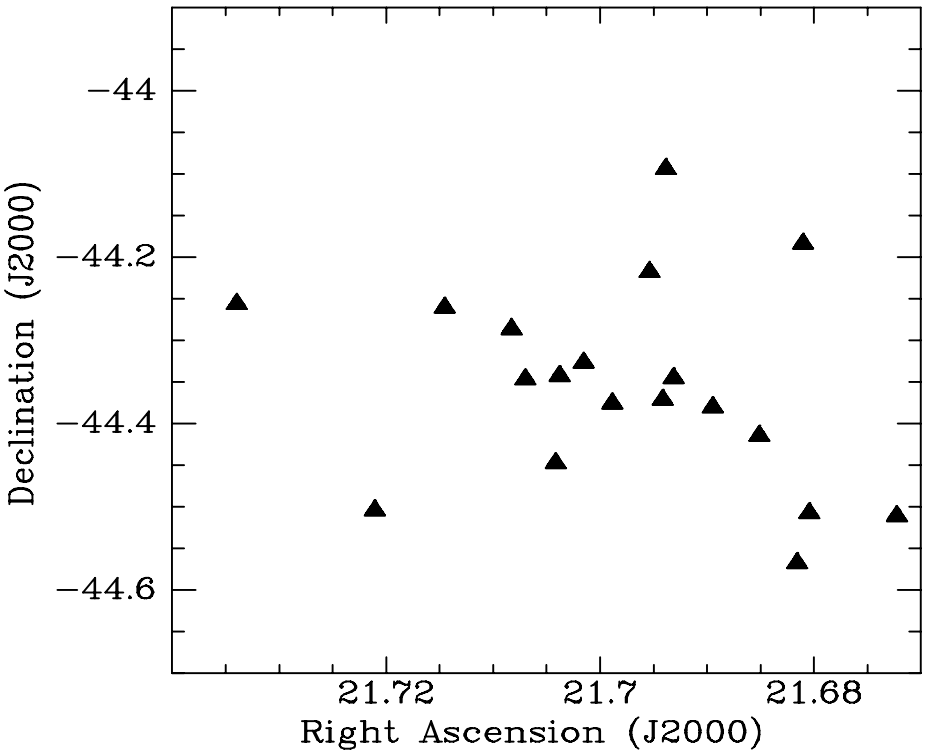

Fig. 8.— Distribution of foreground $z \sim 0.1$, [O II] emitting galaxies in the field.

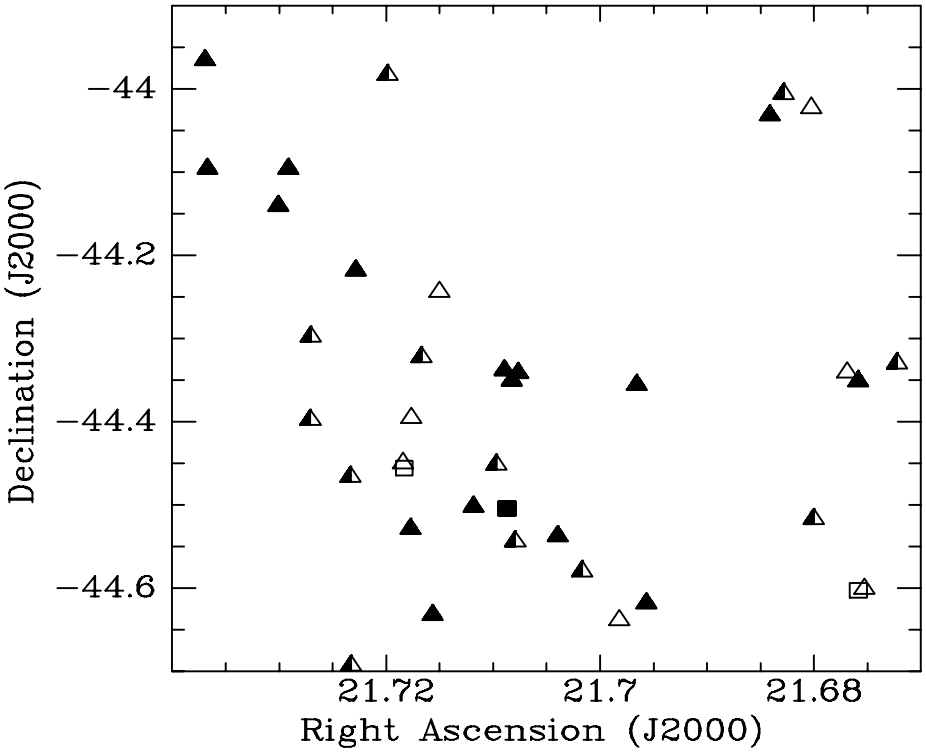

Fig. 9.— Distribution of candidate Lyα emitting galaxies on the sky. Objects with secure spectral confirmations are plotted as solid triangles. Marginal confirmations are shown as half filled triangles, while objects with featureless spectra are empty triangles. The two unobserved candidates are shown as empty squares, and the QSO at the filament redshift as a filled square.

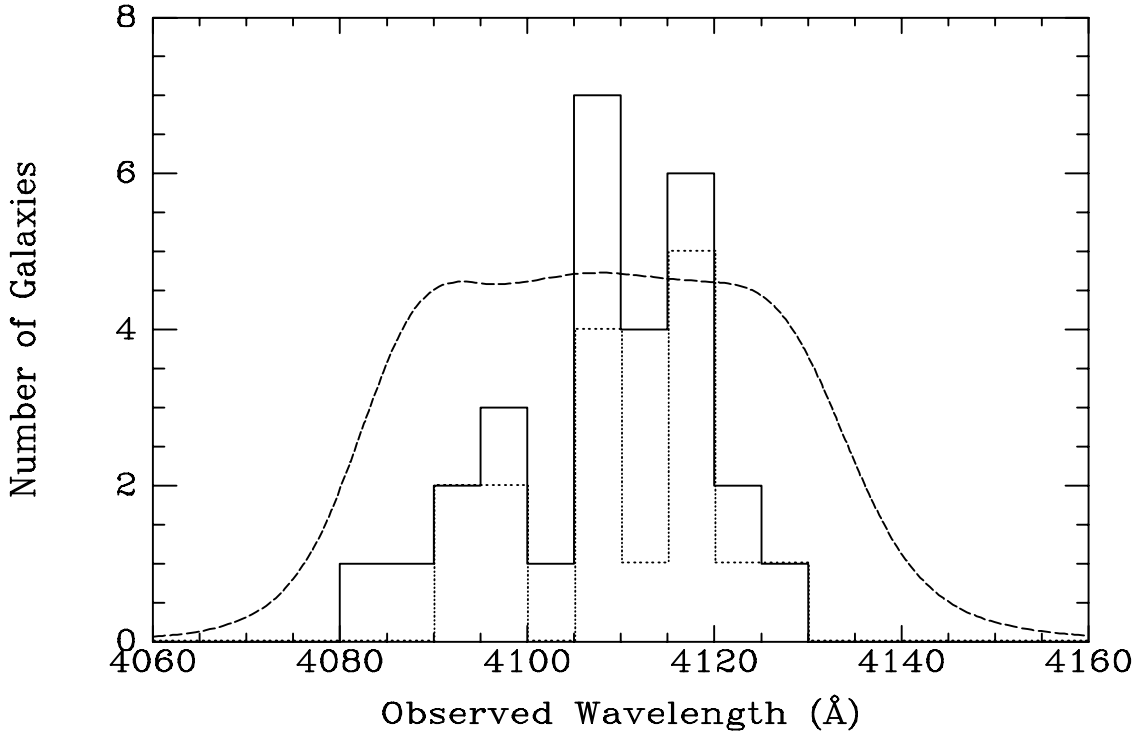

Fig. 10.— Distribution of wavelengths of the secure and marginal Lyα emitting galaxies (solid line) and confirmed sources only (dotted line, slightly offset for clarity), compared to the filter response curve of our narrow-band filter (dashed line), shifted and broadened as appropriate when placed in the converging beam at CTIO prime focus.

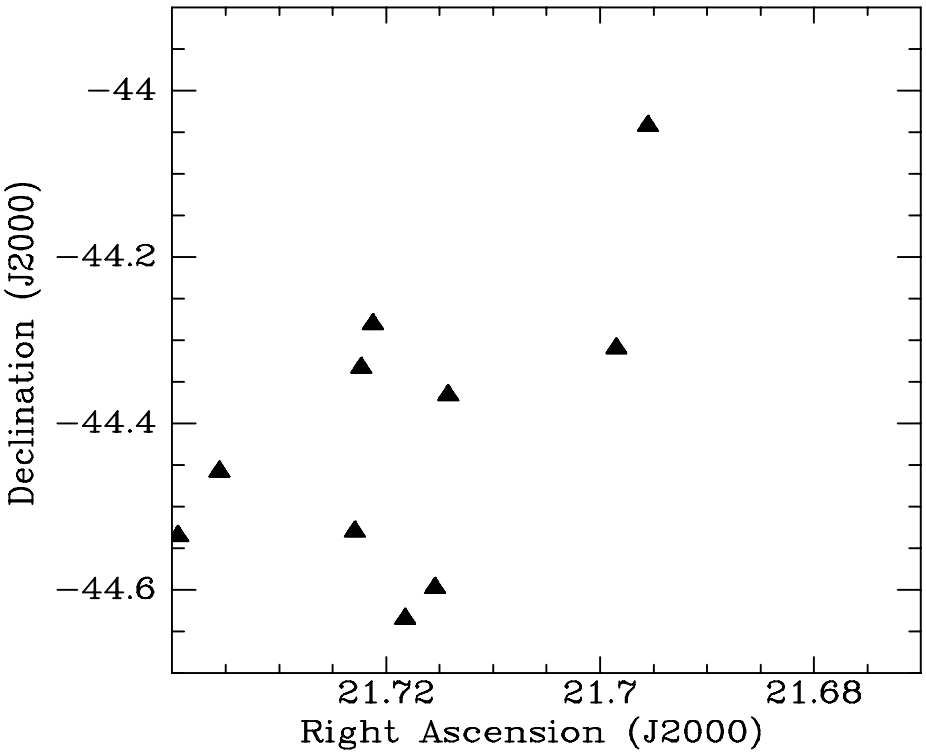

Fig. 11.— Distribution of foreground $1.61 < z < 1.69$ QSOs (QSOs whose C IV line lies within the narrow-band filter passband).

Table 1. Confirmed ($> 5\sigma$) Lyα Emitting Galaxies at z=2.38

Name	Lyα Wavelength	Position (J2000)	NB (mag)	B−NB (mag)	FWHM Lyα km s^{-1}
B1	4113	21:42:27.56 -44:20:30.1	20.97	2.47	900
B2	4109	21:42:29.73 -44:21:02.7	22.86	2.30	<450
B4	4117	21:42:32.20 -44:20:18.6	22.90	2.53	1300
B6	4094	21:42:42.63 -44:30:09.0	22.13	1.89	650
B17	4097	21:41:02.90 -44:01:55.9	22.13	1.89	650
B19	4119	21:41:44.41 -44:37:06.7	22.13	1.89	730
B20	4105	21:41:47.66 -44:21:21.9	22.61	2.37	1200
B23	4116	21:42:14.28 -44:32:15.8	22.18	2.07	700
B26	4117	21:42:56.34 -44:37:56.8	22.48	1.56	<450
B28	4097	21:43:03.80 -44:31:44.9	22.16	2.30	730
B32	4090	21:43 22.22 -44:13:06.5	22.16	2.30	<450
B37	4122	21:43:44.92 -44:05:46.3	22.53	1.66	510
B38	4107	21:43 48.30 -44:08:26.9	22.53	1.66	1400
B39	4106	21:44:12.15 -44:05:46.6	21.46	2.41	880
B40	4116	21:44 12.97 -43:57:56.7	21.46	2.41	1160
b184	4129	21:44:12.15 -44:05:46.6	21 46	2.41	870

Table 2. Possible Lyα Emitting Galaxies at z=2.38 (3 – 5 σ)

Name	Lyα Wavelength	Position (J2000)	NB (mag)	B−NB (mag)
B7	4118	21 42 34.88 -44 27 06.2	21.46	2.41
B10	4082	21:40:19.98 -44:19:48.1	22.62	1.91
B15	4121	21 40 48.09 -44 31 01.7	22.62	1.91
B16	4101	21 40 58.22 -44 00 22.0	22.62	1.91
B22	4107	21:42:06.03 -44:34:47.8	23.18	2.58
B24	4087	21 42 28.54 -44 32 38.5	23.18	2.58
B27	4106	21:43:00.09 -44:19:21.7	22.57	1.70
B31	4110	21:43:11.48 -43:59:01.0	23.13	2.87
B33	4111	21:43:23.80 -44:41:36.4	22.87	1.79
B34	4110	21:43:24.06 -44:27:59.9	22.42	1.81
B35	4097	21:43:37.41 -44:17:53.4	23.21	2.51
B36	4109	21:43:37.47 -44:23:52.8	22.65	2.47

Table 3. QSOs

Position (J2000)	Redshift	B mag	Comment
21:40:13.40 -44:09:18.7	2.045	20.78	
21:40:20.82 -44:32:53.1	1.863	20.69	
21:40:28.71 -43:57:06.9	0.793	20.82	1 liner
21:40:30.12 -44:26:06.3	0.608	22.37	1 liner
21:40:34.91 -44:06:48.3	0.461	23.35	
21:40:39.08 -44:03:07.6	2.097	20.31	
21:40:52.48 -44:36:21.5	0.457	19.96	
21:41:12.32 -44:18:25.7	0.692	22.48	1 liner
21:41:13.25 -44:07:38.3	0.742	21.61	1 liner
In the final paper version, the table will be truncated here and available in electronic format			
21:41:13.67 -43:59:53.9	0.688	22.90	1 liner
21:41:15.43 -43:56:00.7	2.202	21.51	
21:41:18.90 -44:20:42.3	0.714	22.93	1 liner
21:41:22.88 -44:06:48.8	2.106	19.95	
21:41:23.97 -44:33:01.3	0.630	20.27	1 liner
21:41:32.62 -44:25:23.4	0.988	21.35	1 liner
21:41:43.91 -44:02:33.9	1.620	20.06	Foreground cluster
21:41:54.51 -44:18:36.2	1.647	20.14	Foreground cluster
21:41:54.94 -44:42:00.8	2.224	21.89	
21:41:55.73 -44:21:37.4	0.904	20.96	1 liner
21:41:57.61 -44:19:58.8	1.429	20.91	1 liner
21:42:04.05 -44:20:12.5	1.039	21.28	1 liner
21:42:04.90 -44:24:57.5	1.079	19.13	
21:42:07.67 -44:03:10.1	1.732	19.38	
21:42:18.59 -44:08:20.3	1.722	22.88	?
21:42:18.76 -44:15:48.4	1.310	22.00	?
21:42:20.67 -43:59:20.0	2.458	21.59	Background
21:42:21.83 -43:58:11.2	1.112	22.72	?
21:42:25.04 -44:40:02.4	1.458	20.30	?

Table 3—Continued

Position (J2000)	Redshift	B mag	Comment
21:42:29.03 -43:58:38.6	1.853	21.96	
21:42:31.33 -44:30:16.8	2.388	21.24	Filament member
21:42:35.13 -44:32:30.6	0.850	22.34	1 liner
21:42:38.71 -44:06:39.0	1.736	21.10	
21:42:39.38 -44:31:15.2	2.036	22.79	
21:42:43.51 -44:14:25.5	1.589	20.14	
21:42:43.93 -44:32:50.8	1.849	21.44	
21:42:51.15 -44:21:58.9	1.683	21.32	Foreground cluster
21:42:51.50 -44:30:43.2	1.795	20.26	
21:42:55.56 -44:35:52.9	1.639	19.51	Foreground cluster
21:43:05.59 -44:38:06.6	1.638	20.31	Foreground cluster
21:43:11.46 -44:16:20.2	0.664	22.76	1 liner
21:43:12.34 -44:03:35.4	0.984	20.06	
21:43:16.46 -44:16:51.7	1.673	21.71	Foreground cluster
21:43:20.40 -44:20:00.5	1.619	21.05	Foreground cluster
21:43:20.56 -44:04:25.3	1.044	21.62	1 liner
21:43:22.55 -44:31:49.4	1.631	20.86	Foreground cluster
21:43:23.39 -44:35:24.0	2.725	22.02	Background
21:43:23.56 -43:56:38.6	2.223	21.82	
21:43:24.21 -44:04:52.0	1.045	19.44	
21:43:29.62 -44:10:11.9	1.768	21.71	
21:43:32.94 -43:56:31.3	1.557	19.65	
21:43:37.66 -44:08:01.5	2.166	22.02	
21:43:48.73 -44:15:25.1	1.305	22.36	1 liner
21:43:51.26 -44:06:09.6	1.218	22.36	?
21:44:08.11 -44:27:29.8	1.688	20.08	Foreground cluster
21:44:17.56 -44:07:02.0	2.725	21.04	Background
21:44:20.92 -44:23:49.8	2.162	20.49	
21:44:22.04 -44:32:07.9	1.648	20.13	Foreground cluster
21:44:29.09 -44:12:03.4	2.140	22.86	

Table 4. Foreground Galaxies

Position (J2000)	Redshift
21:40:20.15 -44:30:41.9	0.101
21:40:32.69 -44:32:01.2	0.053
21:40:42.82 -44:12:14.6	0.145
21:40:49.58 -44:30:29.2	0.102
21:40:51.69 -44:11:03.5	0.097
21:40:58.13 -44:22:37.6	0.158
21:41:03.10 -44:17:54.0	0.349
21:41:06.21 -44:12:38.0	0.204
21:41:06.42 -44:24:54.8	0.099
21:41:08.66 -44:30:49.1	0.357
In the paper version, the table will be truncated here and available in electronic format	
21:41:10.20 -44:29:21.5	0.055
21:41:19.34 -44:12:56.5	0.062
21:41:22.07 -44:22:51.2	0.104
21:41:34.76 -44:02:12.1	0.353
21:41:35.24 -44:20:45.5	0.097
21:41:37.88 -44:05:40.3	0.102
21:41:37.99 -44:29:43.8	0.094
21:41:38.90 -44:22:18.8	0.103
21:41:43.34 -44:13:06.1	0.102
21:41:48.01 -44:16:15.8	0.317
21:41:48.28 -44:17:34.1	0.328
21:41:54.00 -44:14:29.3	0.055
21:41:55.90 -44:22:34.8	0.094
21:42:02.79 -44:14:44.2	0.311
21:42:05.50 -44:19:38.5	0.102
21:42:12.15 -44:14:53.7	0.566
21:42:13.63 -44:20:35.2	0.099
21:42:14.27 -44:29:11.3	0.264

Table 4—Continued

Position (J2000)	Redshift
21:42:14.95 -44:26:53.1	0.099
21:42:25.12 -44:20:50.3	0.098
21:42:25.39 -44:10:40.7	0.406
21:42:29.36 -44:03:27.7	0.470
21:42:29.82 -44:17:12.8	0.099
21:42:40.54 -44:22:22.7	0.562
21:42:40.97 -43:58:15.5	0.510
21:42:51.39 -43:58:16.6	0.137
21:42:52.30 -44:15:40.2	0.101
21:42:56.55 -43:59:23.5	0.143
21:43:06.10 -43:59:04.2	0.462
21:43:15.81 -44:30:17.3	0.100
21:43:27.59 -44:27:52.0	0.420
21:43:34.40 -44:42:55.6	0.038
21:44:02.26 -44:15:24.1	0.100